Journal of Optics
https://doi.org/10.1007/s12596-024-01828-8

RESEARCH ARTICLE

Physical investigations: structural, morphological, optical and electrical properties of $CoFeS_2$ thin films prepared using a chemical spray technique

A. Mhamdi[1,2]

Received: 12 February 2024 / Accepted: 31 March 2024

Abstract

In this work, Cobalt-iron sulfide ($CoFeS_2$) thin film was deposited on glass substrate at 300 °C using a chemical spray pyrolysis technique. The X-ray diffraction (XRD) investigation reveals that this film is polycrystalline, with a crystallite sizes equal to 86 nm. In addition, the XRD spectra and Energy-Dispersive X-ray analysis (EDXA) illustrate the appearance of $CoFeS_2$, while scanning electron microscopy (SEM) exhibits a surface shape that is largely flat. The optical characteristics of thin films are investigated using ultraviolet–visible (UV–vis) spectroscopy. As demonstrated by the results, $CoFeS_2$ thin films exhibit a high absorption coefficient $\boldsymbol{\alpha}$ in the visible wavelength ($\boldsymbol{\alpha} \geq 10^6$ cm^{-1}). The gap energy $\boldsymbol{Eg}$ of the film is equal to 2.49 eV. Finally, a Hall measurement device using the Vander Pauw method was used to measure electrical resistivity, Hall mobility, and carrier concentration at room temperature.

Keywords $CoFeS_2$ · Thin film · Spray pyrolysis · Physical study · Hall mability

Introduction

For the purpose of resolving the energy crisis, preventing climate change, and lowering local air pollution, it is essential to develop energy storage devices with high specific power and environmental friendliness. With growing consumption and demand linked to industrial development, global energy production is largely dominated by fossil energy (coal, oil, gas). Additionally, the various components of today's wireless technologies must be fueled by effective energy storage devices while having smaller dimensions because they are vital to our everyday lives and are becoming more energy-intensive. The most popular storage option is a battery, which has a significant energy capacity. Batteries use faradic storage techniques, which slow down their charges and discharges, make them unsuitable with high-power systems like quick data transmission. Also, they have a short lifespan.

The supercapacitor is one of the best electrochemical storage gadgets. For this reason, the limitations of batteries could be overcome through the use of micro-supercapacitors. Similar to their larger counterparts, they are used when high power peaks, good cycling stability, and high efficiency between charge and discharge are required. They can be utilized alone as a power source, in conjunction with microbatteries to extend their battery life, or in conjunction with ambient energy harvesters (photovoltaic cells, thermoelectric cells, vibrational energy harvesters, etc.) to provide energy sources and self-sufficient power. Supercapacitors can be divided into electrochemical double-layer capacitors, pseudocapacitors, and battery-like materials based on their electrochemical charge storage method. Many scientists have discovered in recent years that electrode materials have electrochemical characteristics akin to batteries.

We should be aware that $CoFeS_2$ with a hexagonal phase is one of the components that are crucial for battery or supercapacitor applications. The relevance of these materials in several application areas has led to a major surge of interest

✉ A. Mhamdi
ammar.mhamdi@su.edu.sa

[1] Department of Natural and Applied Sciences, College of Science and Humanities Afif, Shaqra University, Afif, Saudi Arabia

[2] Laboratoire de Nanomatériaux, Nanotechnologie et Energie (L2NE), Faculté des Sciences de Tunis, Tunis El Manar University, P. O. Box: 2092, Tunis, Tunisia

in recent years. In fact, $CoFeS_2$ has been the material preferred for the majority of applications, including solar cells [1–3], electrocatalysts [4–7], supercapacitors [8], photocatalysts [9], potassium-ion batteries [10], sodium-ion batteries [6, 11, 12], and lithium-ion batteries [13, 14]. In the majority of these works, $CoFeS_2$ powder is produced using the hydrothermal approach [1–19]. However, in this study, we used a chemical method known as "spray pyrolysis" to create the $CoFeS_2$ thin films. The obtained layers are analyzed using specialized methods including X-ray diffraction, SEM scanning electron microscopy, UV-Visible Spectrophotometry, and the four-point approach. The current study shows that $FeCoS_2$ thin films have a wide range of possible uses in contemporary materials science and technology.

Experimental details

On glass substrates, a thin coating of cobalt-iron-sulfide ($CoFeS_2$) was created by spraying an aqueous solution containing the following precursors: thiourea ($SC(NH_2)_2$) 4.10^{-2} M, Cobalt(II) chloride ($CoCl_2.6H_2O$) 10^{-2} M and Iron(III) chloride ($FeCl_3.6H_2O$) 10^{-2} M as sulfur, cobalt and iron sources, respectively. The flow rates of the solution and nitrogen gas were maintained constant at 2 $cm^3.min^{-1}$ and 5 $l.min^{-1}$, respectively. To create these films, the substrate temperature Ts was set to around 350 °C. Consequently, X-ray diffraction measurements of $CoFeS_2$ films were produced by a copper-source diffractometer (Analytical X Pert PROMPD) with the wavelength $\lambda = 1.5418Å$. Next, the surface morphology of the layer was performed by a JEOL-JSM 5400 model scanning electron microscope (SEM). The optical properties of the deposited layers were assessed at normal incidence in the wavelength range of 250 to 1800 nm using a twin-beam UV-VIS-NIR spectrophotometer (Shimadzu).

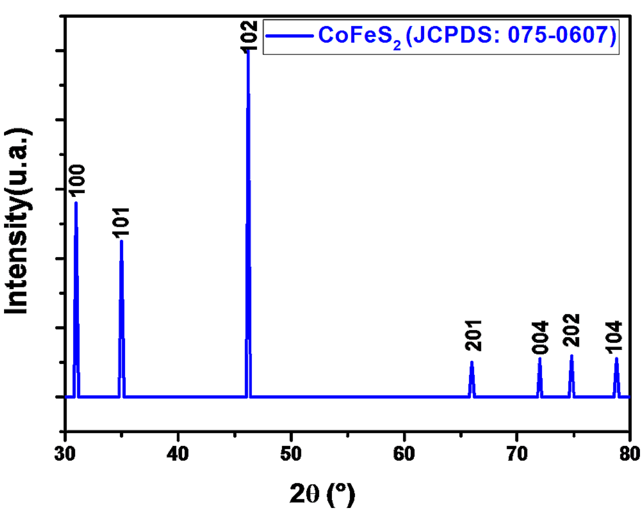

Fig. 1 X-ray difractogram of $CoFeS_2$-sprayed thin film

Finally, a Hall measurement device using the Vander Pauw method was used to detect electrical resistivity, Hall mobility, and carrier concentration at room temperature.

Results and discussion

Structural studies

The XRD spectrum for the $CoFeS_2$ thin film is displayed in Fig. 1, indicating that it is polycrystalline structure. Several high-intensity peaks appear at $2\theta = 30.95°$, 35.12° and 46.32° corresponding to planes (100), (101), (102) and lower intensities at 66.05°, 71.93°, 74.87° and 78.78° corresponding to planes (201), (004), (202) and (104), respectively. In accordance with the JCPDS card N0:75–0607 [1, 8], all diffraction peaks can be accurately indexed as a pure hexagonal structure of $CoFeS_2$ (Fig. 2).

Furthermore, the Debye-Scherrer equation [20] was utilized to determine the crystallite size $\boldsymbol{D}$ of $CoFeS_2$ thin films:

$$D = \frac{K\lambda}{\beta cos\theta} \quad (1)$$

Where $\boldsymbol{\theta}$ is the Braggs angle of diffraction peaks, $\boldsymbol{K} = 0.9$ and $\boldsymbol{\beta}$ is its FWHM. The estimated crystallite size is around 86 nm.

Finally, the following equation [21] is used to determine the microstrain ($\boldsymbol{\delta}$) and dislocation density ($\boldsymbol{\xi}$), which are relevant structural properties of $CoFeS_2$ sprayed thin film:

$$\delta = \frac{1}{D^2} \quad (2)$$

$$\xi = \frac{\beta}{4tg\theta} \quad (3)$$

The values of crystalline size, density of dislocation and the microstrain are given in Table 1.

Morphological properties

Figure 3 shows a typical SEM image of sprayed $CoFeS_2$ thin films. It can be seen in this image that the sample of $CoFeS_2$ is continuous, fairly homogeneous and with little surface roughness. The average grain size is also visualized by SEM is around 80–90 nm.

Additionally, EDX measurements were used to characterize the $CoFeS_2$ thin film (Fig. 4). The principally observed peaks in the spectra are: Co, Fe and S peaks. The other materials are originated from the glass substrate. The atom

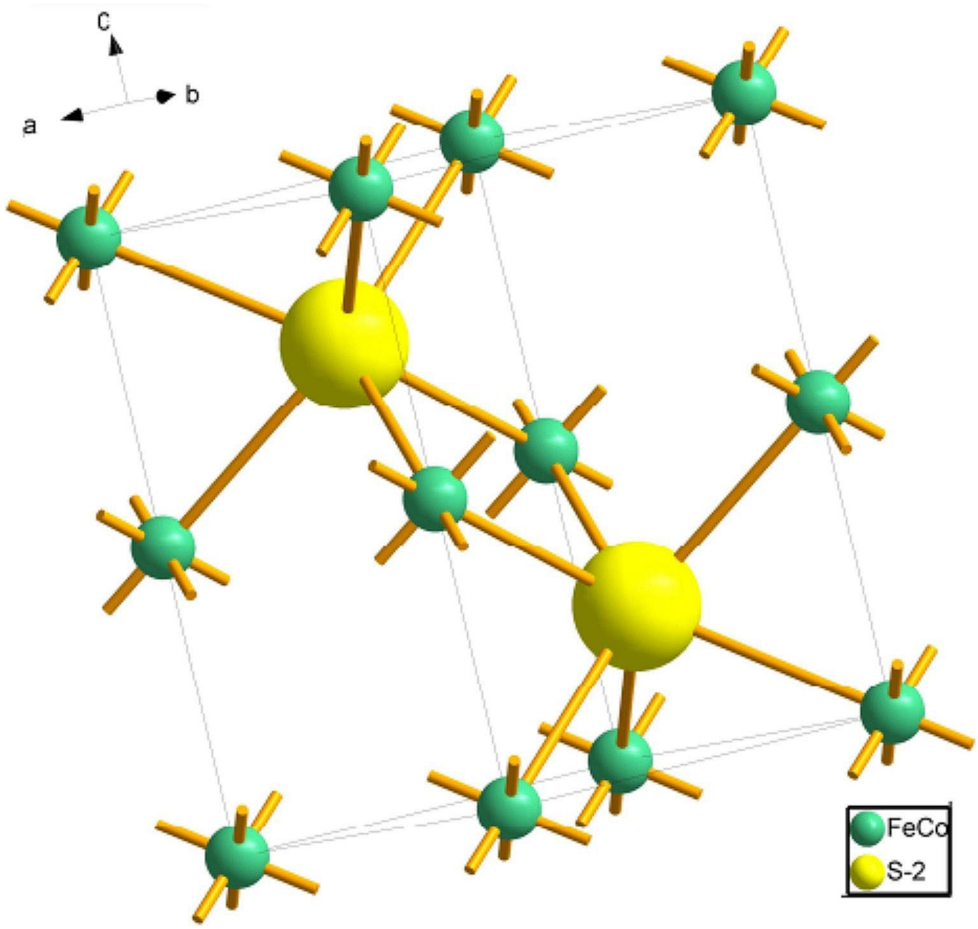

Fig. 2 The crystal structure of $CoFeS_2$

Table 1 The values of crystalline size D, density of dislocation ξ and the microstrain $\boldsymbol{\delta}$

	D (nm)	δ (10^{-4})	ξ
$CoFeS_2$	86	1.35	0.056

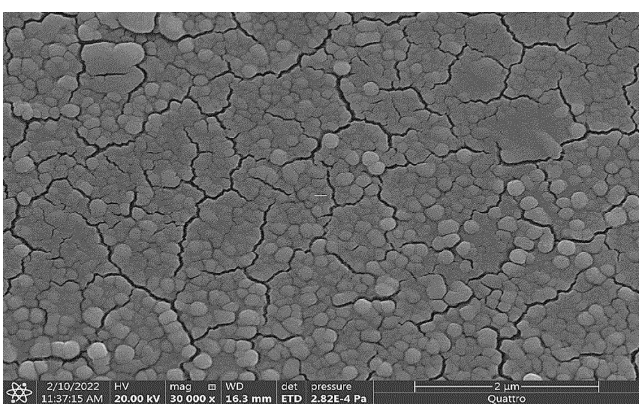

Fig. 3 SEM micrograph of $CoFeS_2$ thin film

concentrations for S, Fe, and Co were found to be 47.69%, 25.62%, and 26.79%, respectively, in the quantitative analysis of the major peaks. This clearly confirms that we obtain $CoFeS_2$ in a thin layer. These results are in perfect agreement with X-ray diffraction (XRD) results.

Optical studies

The transmittance (***T***) and the reflectance (***R***) spectra for the wavelength, which ranged from 250 to 1800 nm, are showed in Fig. 5. In the transparent zone, the transmittance values ranged from 30 to 50%. Additionally, the sample has reflectance levels between 20 and 30% between the wavelengths of 700 and 1800 nm.

Using the transmittance (***T***) and reflectance (***R***) values, the absorption coefficient of $CoFeS_2$ films was determined using the following formula [20]:

$$\boldsymbol{\alpha} = \frac{1}{\boldsymbol{d}} * \boldsymbol{Ln}\left[\frac{(1-\boldsymbol{R})^2}{\boldsymbol{T}^2}\right] \tag{4}$$

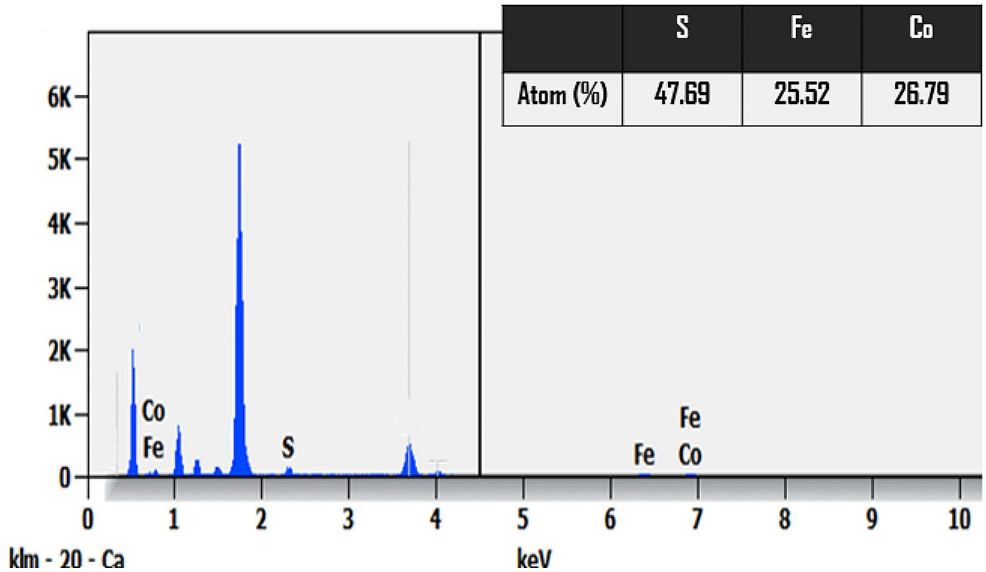

Fig. 4 EDX measurements of $CoFeS_2$ thin film

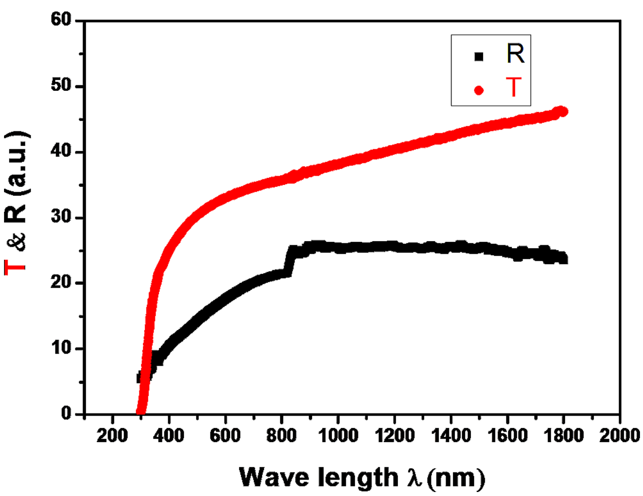

Fig. 5 The spectral transmittance (***T***) and reflectance (***R***) of $CoFeS_2$ thin film

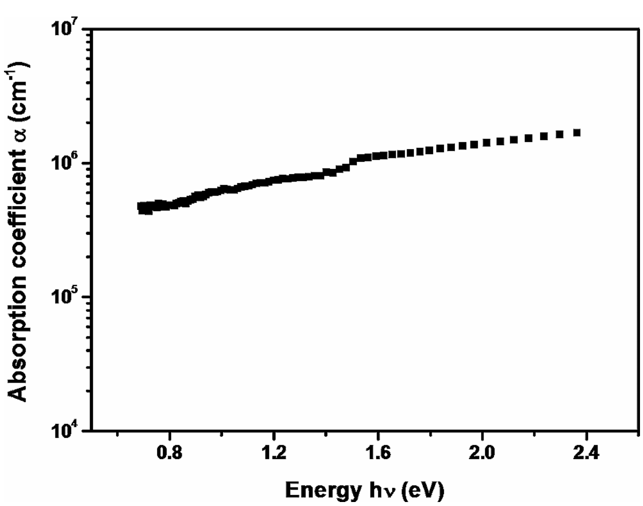

Fig. 6 Absorption spectra of sprayed $CoFeS_2$ thin film

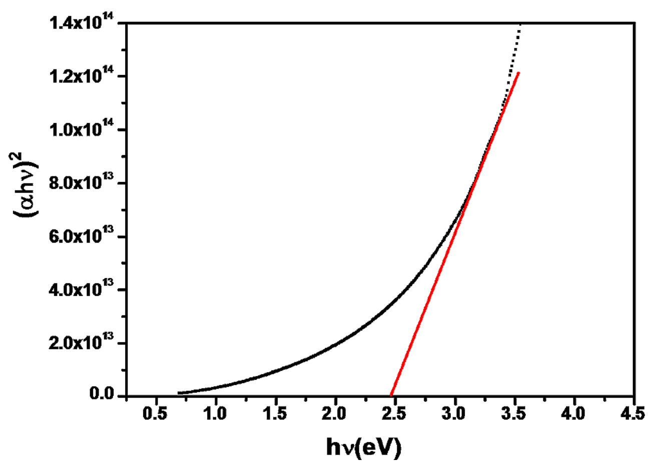

Fig. 7 Plots of $(\alpha h\nu)^2$ versus the photon energy of Cobalt-iron sulfide layer

where ***d*** is the thickness of this layer, ***R*** and ***T*** are the reflection and transmission coefficient, respectively. Figure 6 illustrates the effects of the absorption coefficient on photon energy for the $CoFeS_2$ thin film. In the visible and near-IR spectral regions, the sample shows comparatively large absorption coefficients, exceeding 10^6 cm^{-1}. So the spectral dependency of the absorption coefficient may significantly impair the solar energy conversion efficiency, even if such a high value of absorption coefficient may be advantageous for the production of high absorptive layers of solar cells [3, 7].

As shown in Fig. 7, the linear nature of the $(\alpha h\nu)^2$ plots in the mean absorption range, along the photon energy ($h\nu$) axis, indicates that the electronic transitions are direct. The following relationship [20] was used to determine the optical band gap ***Eg*** values based on the intersection of this linear sections slope:

Table 2 The hall effect measurements of Cobalt-iron sulfide thin film

	Conductivity-type	Carrier concentration n (cm^{-3})	Resistivity ρ (Ω.cm)	μ (cm^2/V.S)
$FeCoS_2$	**p- type**	**2.71 10^{20}**	**4.52 10^{-2}**	**0.50**

$$(\alpha h\nu)^2 = A(h\nu - E_g) \tag{5}$$

Where ***A*** is the semiconductor's constant property. The band gap ***Eg*** of the films equals to 2.49 eV. The measured value of ***Eg***, as opposed to CdS buffer layer with a direct optical band gap of 2.4 eV [22], indicates that $CoFeS_2$ thin layer could be utilized as an efficient buffer layer material for thin film solar cells.

Hall effect studies

When applying the Hall effect to a semiconductor carrying a current and a magnetic field perpendicular to this current, an electric field appears perpendicular to the direction of transport and to the magnetic field. Measuring the potential difference (Hall voltage) corresponding to this electric field makes it possible to determine the concentration of charge carriers as well as their nature (electrons or holes). By combining this measurement with that of resistivity, we can also determine their mobility. Table 2 presents the results of the Hall effect measurements, which were performed at room temperature in a Van der Pauw four-point arrangement. In our study, we found that $CoFeS_2$ thin film exhibit ***p***-type conductivity. In addition, we noted a low resistivity value equal to 1.32 Ω.cm. It demonstrates the system's potential for solar application.

Conclusions

In this work, we prepared CoFeS2 thin films by spray pyrolysis and examined the physical properties of these thin layers. We discovered that the thin film has a hexagonal structure. The optical studies show that the FeCoS2 thin film is opaque, and the gap energy is equal to 2.49 eV. Based on the Hall effect measurements, ***p***-type conductivity in the CoFeS2 thin film was found. Also, we noticed a low resistance value. Our conclusions were based on these data, which suggested that the CoFeS2 thin layer would be a strong contender in the photovoltaic field. It is obvious that further research on this topic has to be done in the future.

Acknowledgements The author would like to thank the Deanship of Scientific Research at Shaqra University for supporting this work.

References

1. W. Yuan Gao, W. Liao, X. Wang, Q. Zuo, H. Yang, S. Tang, Jin, G. Li, FeS_2/$FeCoS_2$ nanoparticles/reduced graphene oxide interfacial composite structure as highly reactive counter electrodes in dye-sensitized solar cells. J. Mater. Sci: Mater. Electron. **32**, 8226–8236 (2021)
2. Y. Wang, S. Wang, S.L. Zhang, D.X. Lou, W.,formation of hierarchical $FeCoS_2CoS_2$ doubleshelled nanotubes with enhanced performance for photocatalytic reduction of CO2. Angew Chem. Int. Ed. Eng. **59**, 11918–11922 (2020)
3. R. Qin Wu, P. Chen, D. Su, Y. Shi, K. Zhang, H. Che, Li, Co_9S_8/NC@$FeCoS_2$/NC composites with hollow yolk shell structure as the counter electrode for Pt-free dye-sensitized solar cells. Electrochim. Acta. **438**, 141587 (2023)
4. X. Shuliang Wang, S. He, X. Wang, M. Huang, D. Wu, Xiang, $FeCoS_2$/Co_4S_3/N-doped graphene composite as efficient electrocatalysts for overall water splitting. Electrochim. Acta. **441**, 141790 (2023)
5. D. Zeen Wang, K. Pan, X. Chen, J. Yin, P. Wang, Cai, Z. Wen, Palladium modified $FeCoS_2$ nanosheet arrays on Ni Foam as Bifunctional Electrodes for overall Alkaline Water Splitting. Chem. Select. **8**, 20220445 (2023)
6. Y.-G. Xu, J. Liu, L.-B. Kong, Fe-doped CoS_2 nanospheres decorated by reduced graphene oxide nanosheets as ultrahigh-rate anodes for advanced sodium-ion capacitors. J. Electroanal. Chem. **901**, 115740 (2021)
7. Z. Zhang, J. Zhou, H. Wei, Y. Dai, S. Li, Haojun Shi, Gang, Xu, Construction of hierarchical NiFe-LDH/$FeCoS_2$/CFC composites as efficient bifunctional electrocatalysts for hydrogen and oxygen evolution reaction. J. Mater. Sci. **55**, 16625–16640 (2020)
8. M. Guo, X. Li, X. Liu, H. Pan, K. Wu, Y. Xue, B. Li, Y. Cao, Facile Fabrication of Iron Cobalt Sulfide nanoparticles within NDoped Graphene for High-Performance Supercapacitors, ACS Appl. Nano Mater. **5**, 16553–16563 (2022)
9. F. Zhao, H. Miao, J. Fan, T. Sun, C. Tang, E. Liu, Fabrication of S-scheme FeCoS2/Red phosphorus heterojunction for efficient photocatalytic H_2 evolution. Colloids Surf., a **676**, 132316 (2023)
10. H. Xu, S. Huang, Y. Yang, J. Chen, L. Liang, J. Zhang, L. Li, X. Zhao, W. Zhang, $FeCoS_2$ polyhedral spherical nanoparticle decorated nitrogen doped hollow carbon nanofibers as high-performance self-supporting anodes for K-ion storage. Dalton Trans. **51**, 16126–16134 (2022)
11. X. Chen, N. Cheng, L. Zhang, G. Xiang, Y.-L. Ding, Z. Liu, Flower-like spherical $FeCoS_2$ coated by reduced graphene oxide as anode for high performance potassium ion storage. J. Alloys Compd. **861**, 158458 (2021)
12. Y. Zhao, J. Liu, C. Ding, C. Wang, X. Zhai, J. Li, H. Jin, The synthesis of $FeCoS_2$ and an insight into its physicochemical performance. Cryst. Eng. Comm. **20**, 2175–2182 (2018)
13. J. Tian Gan, Y. Wang, Z. Liao, F. Lin, Wu, Catalytic performance of binary transition metal sulfide FeCoS2/rGO for lithium–sulfur batteries. J. Solid State Electrochem. **27**, 1045–1053 (2023)
14. M.M.N. Nesrin Buğday, O. Ates, W. Duygulu, X. Deng, S. Ji, Altin, Sedat Yaşar, ZIF-12-derived N-doped Fe/Co/S/@C nanoparticles as high-performance composite anode electrode materials for lithium-ion batteries. J. Alloys Compd. **928**, 167037 (2022)
15. W. Yanru Wang, C. Jin, J. Xuan, J. Wang, Q. Li, B. Yu, C. Li, W. Wang, J. Cai, Wang, In-situ growth of CoFeS2 on metal-organic frameworks-derived Co-NC polyhedron enables

high-performance oxygen electrocatalysis for rechargeable zinc-air batteries. J. Power Sources. **512**, 230430 (2021)
16. C. Zhao, J. Dai, Z. Lu, R.F.F. Zhu, J. Wu, Y. Cai, FeCoS2 nanoparticles confined in N, S co-doped carbon with reduced polysulfides shuttling for high performance sodium-ion batteries. Appl. Surf. Sci. **634**, 157711 (2023)
17. A. Amitha Shetty, M. Saha, Makkar, R. Viswanatha, Ligand assisted digestion and formation of monodisperse FeCoS2 nanocrystals. Phys. Chem. Chem. Phys. **18**, 25887–25892 (2016)
18. Q. Li, S. Tang, Z. Tang, Q. Zhang, W. Yang, Microwave -assisted synthesis of FeCoS2/XC-72 for oxygen evolution reaction. Solid State Sci. **96**, 105968 (2019)
19. R. Cheng, Y. Wang, X. Di, Z. Lu, P. Wang, X. Wu, Heterostructure design of MOFs derived Co9S8/FeCoS2/C composite with efficient microwave absorption and waterproof functions. J. Mater. Sci. Technol. **129**, 15–26 (2022)
20. B. Khalfallah, N. Khemiri, M. Kanzari, Temperature effect on the physical properties of CuIn11S17 thin films for photovoltaic applications. Mater. Sci. Semiconduct. Process. **24**, 265–271 (2014)
21. S. Rajeh, A. Mhamdi, S. Ben Ameur, A. Arfaoui, G. Leroy, B. Duponchel, S. Guermazi, Enhancement of visible light Emission of Ni-Doped ZnO Sprayed Thin films by Copper Co-doping. Prot. Met. Phys. Chem. Surf. **59**, 413–421 (2023)
22. J. Han, C. Spanheimer, G. Haindl, G. Fu, V. Krishnakumar, J. Schaffner, C. Fan, K. Zhao, A. Klein, W. Jaegermann, Optimized chemical bath deposited CdS layers for the improvement of CdTe solar cells, Solar, Energy Mater. Sol Cells. **95**, 816 (2011)